

Nature-Inspired Self-Organization, Control, and Optimization in Heterogeneous Wireless Networks

Haijun Zhang, Jaime Llorca, *Member, IEEE*,
Christopher C. Davis, *Fellow, IEEE*, and Stuart D. Milner, *Member, IEEE*

Abstract—In this paper, we present new models and algorithms for control and optimization of a class of next generation communication networks: Hierarchical Heterogeneous Wireless Networks (HHWNs), under real-world physical constraints. Two biology-inspired techniques, a Flocking Algorithm (FA) and a Particle Swarm Optimizer (PSO), are investigated in this context. Our model is based on the control framework at the physical layer presented previously by the authors. We first develop a nonconvex mathematical model for HHWNs. Second, we propose a new FA for self-organization and control of the backbone nodes in an HHWN by collecting local information from end users. Third, we employ PSO, a widely used artificial intelligence algorithm, to directly optimize the HHWN by collecting global information from the entire system. A comprehensive evaluation measurement during the optimization process is developed. In addition, the relationship between HHWN and FA and the comparison of FA and PSO are discussed, respectively. Our novel framework is examined in various dynamic scenarios. Experimental results demonstrate that FA and PSO both outperform current algorithms for the self-organization and optimization of HHWNs while showing different characteristics with respect to convergence speed and quality of solutions.

Index Terms—Heterogeneous wireless networks, mobile ad hoc networks, directional wireless communication, flocking algorithm, particle swarm.

1 INTRODUCTION

RECENT advances in directional wireless communications for providing mobile, broadband wireless connectivity are making next generation communication networks increasingly complex. These networks are characterized by hierarchical architectures, with heterogeneous properties and dynamic behavior. The need for ubiquitous broadband connectivity and the capacity limitation of homogeneous wireless networks [1] is driving communication networks to adopt hierarchical architectures with diverse communication technologies and node capabilities at different layers that provide assured end-to-end broadband connectivity in a wide range of scenarios [2], [3], [4], [5], [6], [7]. In particular, Hierarchical Heterogeneous Wireless Networks (HHWNs) use a wireless backbone network consisting of a set of base stations or backbone nodes that use directional wireless communications to provide end-to-end broadband connectivity to capacity-limited ad hoc networks and/or

end hosts. As an example illustrated in Fig. 1, backbone-based wireless networks use a two-tiered network architecture, which consists of a set of flat ad hoc wireless networks and/or hosts as well as a broadband wireless mesh backbone network of higher capability nodes. In this architecture, backbone nodes use directional wireless communications (higher tier), either Free Space Optical (FSO) or directional Radio Frequency (RF), to aggregate and transport traffic from hosts at lower layers (lower tier). The advantages of directional wireless communications can be well exploited at the upper layer, where line of sight constraints are less restrictive and interference-free, and point-to-point communication links can provide extremely high data rates (up to and beyond Gb/s).

The most important concern in HHWNs is to assure network coverage and backbone connectivity in dynamic wireless environments. Llorca et al. presented a convex energy minimization model for the joint coverage-connectivity optimization problem in HHWNs that dynamically adjusts the location of mobile backbone nodes in order to minimize the potential energy of the network system. The potential energy function for HHWNs is defined as the total communications energy stored in the wireless links forming the network [11], [12]. A completely distributed, gradient-based Force algorithm was presented that drives the network topology to optimal configurations based on local “forces” exerted on network nodes [11], [12].

In this paper, we show that when adding real-world constraints, such as power limitations, the capacity of the base stations and link blockage by terrain, the problem should no longer be formulated as a strictly convex optimization problem. Thus, this research focuses on the modeling of HHWNs under real-world physical constraints,

• H. Zhang is with the Department of Computer Science, Shenzhen Graduate School, Harbin Institute of Technology, University Town Xili, Shenzhen 518055, P.R. China. E-mail: aarhzhang@gmail.com.

• J. Llorca is with the Bell Labs, Alcatel-Lucent, Holmdel, NJ 07733. E-mail: jaime.llorca@alcatel-lucent.com.

• C.C. Davis is with the Department of Electrical and Computer Engineering, University of Maryland, College Park, MD 20742. E-mail: davis@umd.edu.

• S.D. Milner is with the Department of Civil and Environmental Engineering, University of Maryland, College Park, MD 20742. E-mail: milner@umd.edu.

Manuscript received 27 Sept. 2010; revised 9 May 2011; accepted 10 June 2011; published online 8 Aug. 2011.

For information on obtaining reprints of this article, please send e-mail to: tmc@computer.org, and reference IEEECS Log Number TMC-2010-09-0445. Digital Object Identifier no. 10.1109/TMC.2011.141.

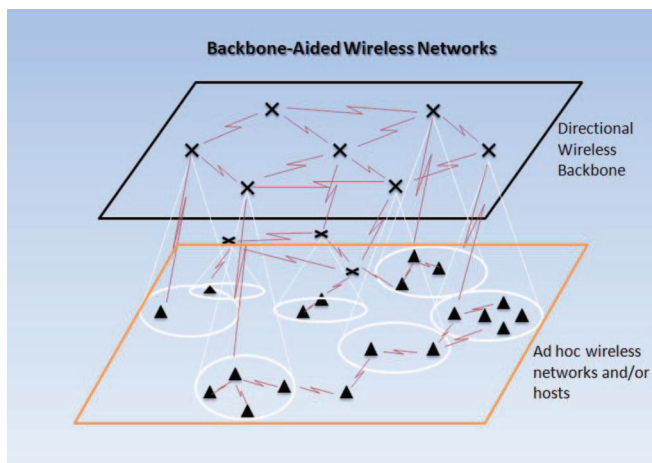


Fig. 1. Two-tiered architecture.

and the development of effective biology-inspired algorithms for topology and mobility control in dynamic scenarios. We compare their performance with the optimal configuration of backbone nodes for the energy minimization problem in an HHWN. The proposed approach delivers a number of desirable features that include generality, robustness, and efficiency. Specifically, these features can be described as follows:

- The model's generality encompasses the hierarchical architecture of wireless communication networks and its modeling methodology under real-world physical constraints. We use a two-tiered backbone-based network architecture (Fig. 1), where a set of flat ad hoc wireless networks with limited capabilities are interconnected through a broadband wireless mesh backbone network of higher capability nodes. This two-tiered architecture can be extended n -fold: the bottom layer can be extended by a heterogeneous set of end users with different communication capabilities, which could be fixed, mobile, or organized in cluster-forming ad hoc networks; and the upper layer can be constructed through multiple hierarchical layers of high capability backbone nodes.
- The proposed approach is robust because of its adaptation to a changing environment and its robustness to real-world physical constraints, which include power limitations, communication capacity, channel limitations such as obscuration and/or atmospheric turbulence, taboo areas (geographic environment, undesirable weather events, security blockages, etc.). The main challenge in the design of Directional Wireless Backbone (DWB) networks is to assure robust network performance in a highly dynamic environment that is characterized by dynamics of end users or nodes (node mobility, node addition, and deletion) and link state (connection path loss, atmospheric attenuation, and turbulence). Our topology control strategies enable us to provide a self-organizing capability to dynamically maintain network performance. By incorporating real-world physical constraints into the network control model, the system energy can be minimized in conjunction with guarantees of maximum end-to-end communication.

- Optimality and speed are two key measures of effective self-organization and optimization algorithms for HHWNs. We are inspired by dynamic models in nature (e.g., flocking and swarming) as they can be applied to the control and self-organization of HHWNs. Our proposed approaches use a Flocking Algorithm (FA) and a Particle Swarm Optimizer (PSO) to deliver optimized dynamic network behavior. The FA-based approach produces optimal solutions from local interactions, is completely distributed and shows constant time complexity, which is especially useful for large-scale HHWNs and real-time applications. The PSO-based approach produces optimal solutions in a stochastic manner, using global network information, which reduces the risk of trapping in local minima while delivering satisfactory computational efficiency.

The new main contributions of this paper are threefold. First, we present a nonconvex model for topology control in HHWNs where the minimization of the potential energy function is subject to real-world physical constraints. Second, we propose a new FA to self-organize the backbone network at the upper layer in order to adapt to changing environments and minimize the system's energy. Third, we employ a PSO algorithm to solve the global optimization problem using a hybrid fitness function. A comparison between FA and PSO in terms of network metrics is discussed to provide insight for further work. This work shows that both FA and PSO outperform our previous force-driven algorithms [2], [12] for the optimization of HHWNs. PSO achieves superior performance in comparison to FA but leads to a relatively slow convergence speed and only favors the dynamics of backbone nodes in an x - y plane. In contrast, FA is capable of delivering fast convergence speed while producing satisfactory solutions for an HHWN. Moreover, the repulsion model used in FA allows backbone nodes to move flexibly in 3D space, satisfying physical constraints (e.g., mountains).

The remaining sections of this paper are organized as follows: a brief overview of heterogeneous wireless networks, flocking algorithms and Particle Swarm Optimization techniques is presented in Section 2. Section 3 describes the problem this research focuses on and the associated mathematical models. In Section 4, we develop and evaluate a new FA for the self-organization and optimization of HHWNs, and the corresponding algorithm is implemented. In Section 5, PSO is employed to solve the global optimization problem in HHWNs using a hybrid objective, and the detailed implementation procedures of the algorithm are described. We conduct extensive experimental verifications in Section 6. A comparison between FA and PSO is discussed in Section 7. Section 8 concludes the paper with suggestions for future work.

2 RELATED WORK

2.1 Evolution of Wireless Networks

Wireless internet protocol-based networks have evolved since the 1990s and can be described as involving three architectures: 1) flat mobile ad hoc networks (e.g., [8]); 2) fixed, base station or infrastructure networks (e.g., [10]); and 3) mobile, dynamic HHWNs (e.g., [2], [3], [4], [5], [6],

[7]). A wireless mobile ad hoc network is a homogeneous, decentralized wireless network consisting of multiple hosts which also act as routers, that support multihop traffic through dynamic wireless links [8]. Although minimal configuration complexity and quick deployment make such ad hoc networks suitable for sensor, surveillance and emergency applications, the overall capacity of such networks is constrained by theoretical [1] and practical [9] limitations. In order to overcome their capacity and scalability limitations, cellular (single-hop) networks use fixed base stations to more efficiently handle routing and multicasting functions, and bandwidth limitations [10]. However, the fixed backbone infrastructure limits network coverage as well as the ability to handle network dynamics such as the mobility of the terminal nodes and the dynamics of the wireless channel. In [2], [3], [4], [5], [6], and [7], an HHWN architecture was introduced.

Llorca et al. [11] first proposed a quadratic optimization method to jointly control network coverage and backbone connectivity. They defined a quadratic energy function to characterize the robustness of HHWNs and designed a force-driven algorithm that dynamically drives the network topology to minimum energy configurations based on local forces exerted on network nodes. A quadratic model of the energy function was then extended to an exponential model that takes into account the effects of atmospheric attenuation on the propagation of electromagnetic energy in directional wireless links [12]. The convex energy model was used by the authors to develop an Attraction Force Driven (AFD) algorithm, where the net force used to relocate the backbone nodes is computed as the negative gradient of the energy function at the backbone nodes locations. By considering practical power limitation constraints at the network nodes, recently Llorca et al. [2] further extended the energy model using the Morse potential [13], such that the convex energy function [12] was transformed into a nonconvex function where communication energy saturates with distance emulating the effects of link failure as a result of power limitation constraints. Based on this nonconvex energy model, Llorca et al. developed a hybrid control model where communication links are retained or released autonomously based on their cost within the network architecture [2].

While these models take into account some constraints on communication links such as transmitted power limitations, a comprehensive model for topology control with real-world physical constraints such as taboo areas needs to be developed and validated. In addition, the modeling of dynamics and heterogeneity needs investigation in a fully mobile HHWN. Recently, Liu et al. [14] proposed a topology control method for a multichannel multiradio wireless network using directional antennas. However, their method is based on the adjustment of antenna orientations and channel assignment in static mesh router configurations, while our topology control strategies consider the dynamic movement of base station nodes at the physical layer of an HHWN. The use of mobility to improve network performance has been considered in the context of ad hoc wireless networks. In [15], Grossglauser and Tse exploit multiuser diversity by using mobile nodes as relays in order to scale throughput while still restricting transmission to close neighborhoods. While an end user's mobility

cannot be controlled, a backbone or set of mobile base stations at the higher tier can be. Accordingly, in our work, mobility is controlled at the backbone layer to dynamically optimize base station node movements in order to maximize coverage of end users, while maintaining backbone connectivity.

2.2 Flocking Models of Dynamic Behavior in Nature

We are investigating how to apply flocking models, which have been derived from observations in nature, such as the dynamic movements of birds and other airborne animals, to the self-organization and control of backbone nodes in an HHWN.

Previous work on flocking is derived from the animation of the birds' flocking dynamics. Reynolds et al. [16], [17] developed a basic flocking model using three simple steering rules to control individual agents in the flock. These steering rules [16], [17] include

- **Alignment.** Steering to move toward the average heading of neighboring flock mates.
- **Separation.** Steering to avoid collision with other local flock mates.
- **Cohesion.** Steering to move toward the average position of neighboring flock mates.

The size of a neighborhood is determined by the sensor range of a flocking agent. Since the movement of an agent is only based on local information, the computational time complexity is significantly reduced. These three rules in Reynolds's model [17] are sufficient to emulate the group behavior in nature. This flocking model has been widely applied in data visualization [18], [19] and clustering [20], [21], [22]. Apart from Reynolds's model and its applications, the dynamics of biological systems have also drawn high attention in other research fields such as physics, control engineering, and biology. Vicsek et al. [23] first proposed a phase transition model to investigate the emergence of self-ordered motion in systems of particles with a biologically inspired interaction. Jadbabaie et al. [24] and Moreau [25] conducted a stability analysis with respect to Vicsek's model [23]. Gazi and Passino [26], [27] later proposed a model using a continuous function to model the attraction and repulsion between agents. Another model was also introduced to analyze the information distribution in animal groups [28]. Many flocking control algorithms such as predictive control [29] also have been investigated. One advantage of these flocking models is the fact that they work in a completely controlled way such that the system complexity is reduced. In addition, the models do not need any prior knowledge because the agents in the model are force driven in a heuristic way. If the flocking space is continuous and no physical constraints are imposed, the coordination (convergence) of a group of agents can be achieved [24], [25], [26], [27]. It is worth noting that most studies of flocking in the control field only focus on the topology of one leader and multiple followers and its stability analysis. In real applications, however, many practical constraints, e.g., undesired weather events, geographic conditions, and information capacity of each agent, should be considered. We investigate more complex systems consisting of multiple leaders (hosts) and multiple

followers (backbone nodes). Thus, since the movement of each agent is only based on local information, it is difficult to reach the globally optimal state for the entire system.

2.3 Particle Swarm Optimization

We are also investigating how to apply what has been learned about global, dynamic, and complex behavior in animals in nature to the self-organization of HHWNs.

PSO, as proposed by Kennedy and Eberhart [30], is inspired by biological behaviors such as birds flocking and fish schooling. In PSO, each individual, referred to as a particle, is denoted as part of a solution to the optimization problem and is assigned a randomized velocity. The particle changes its position and velocity gradually by following its own local optimum and the global optimum, in other words, according to its own experience and the whole swarm experience. Therefore, it is a stochastic global optimization algorithm. Compared with other evolutionary algorithms, PSO has some appealing features including easy implementation, few parameter tuning and a fast convergence rate. It has been used in a wide variety of applications such as neural network learning, pattern recognition, data mining, controller design, and circuit optimization [31], [32], [33], [34], [35]. A single-objective and unconstrained optimization problem can be simply formulated as

$$\text{Min}f(\mathbf{X}), (\mathbf{X} \in \Omega, \mathbf{X} = (x_1, x_2, \dots, x_d)), \quad (1)$$

where Ω is denoted as the hyperspace and d is the dimension of the optimization problem (in this paper, we only discuss the minimization problem). A particle in the search space is characterized by two parameters: position and velocity. The position and the velocity of the l th particle in the d -dimensional search space can be represented as $X_l = (x_{l,1}, x_{l,2}, \dots, x_{l,d})$ and $V_l = (v_{l,1}, v_{l,2}, \dots, v_{l,d})$, respectively. The l th particle has its own best position (local optimum) $P_l = (p_{l,1}, p_{l,2}, \dots, p_{l,d})$ corresponding to the individual optimum obtained so far at time t . The global best position is denoted by $G = (g_1, g_2, \dots, g_d)$, which represents the best position found so far at time t for the whole swarm. The new velocity of each particle is given by [30]

$$V_l(t+1) = wV_l(t) + c_1r_1[P_l - X_l(t)] + c_2r_2[G - X_l(t)], \quad (2)$$

where c_1 and c_2 are constants denoted as acceleration coefficients (usually $c_1 = c_2 = 1.49$), r_1 and r_2 are two independent random numbers uniformly distributed in the range $[0, 1]$, w is the inertial weight. Empirical studies [36] suggest that the convergence performance can be greatly improved if $w \in [0.4, 0.9]$ declines linearly as the exploration proceeds. The updating scheme is given by

$$w(t) = w_{\max} - t \times \frac{(w_{\max} - w_{\min})}{t_{\max}}, \quad (3)$$

where w_{\max} and w_{\min} are the maximum and minimum inertial weights, respectively, and t_{\max} is the maximum number of iterations. The position of each particle is then updated according to

$$X_l(t+1) = X_l(t) + V_l(t+1). \quad (4)$$

Usually the value of each component in V_i is constrained to the range $[v_{\min}, v_{\max}]$ in order to control the excessive

roaming of particles outside the search space. Particles move toward new positions according to (4). This process repeats until either the maximum number of iterations is reached or the stopping criterion is satisfied.

2.4 Flocking and Particle Swarm for Optimization and Control in HHWNs

The objective with respect to the control of HHWNs is to minimize the network energy by relocating the positions of the backbone nodes and adapting to the network dynamics under real-world physical constraints. Two algorithmic methods—FA and PSO—are proposed to solve the energy minimization problem such that the HHWN is autonomously self-organized and optimized. There is a strong rationale behind using these two different approaches.

The relationship between HHWNs and flocking is described by the following analogs:

- **Entity.** Terminal nodes (leaders) lead the backbone nodes (followers) in HHWNs; in FA, each agent or assigned leader leads its neighboring agents.
- **Control object.** Backbone nodes are the control objects in the HHWN, while each agent (except the group leader) needs to be controlled in FA.
- **Interaction.** In an HHWN, each backbone node interacts with its neighboring backbone nodes, assigned terminal nodes, and physical constraints, e.g., geographic constraints and undesired weather conditions (we will specifically explain these constraints in the subsequent section); in FA, each agent only interacts with its neighboring agents.
- **Optimum.** In an HHWN, the energy, which includes the costs of connectivity (the links between backbone nodes) and coverage (the links between backbone nodes and terminal nodes), needs to be minimized under physical constraints; each agent in FA interacts with its neighboring agents in order to make the whole flocking group reach an optimal state, where the whole system is well self-organized and optimized.

On the other hand, PSO uses a stochastic global optimization method, which can be directly used to optimize the energy (connectivity and coverage) of HHWNs. Since the optimal solution with respect to HHWNs is the best location of each backbone node for the current state of terminal nodes, it is straightforward to encode each particle in PSO as the locations of all the backbone nodes. Thus, according to (4) each particle moves based on an evaluation function (e.g., the energy function) to maintain the connectivity and coverage jointly, but it needs to collect global information from all the backbones.

We will discuss the relationship between FA and PSO together with a thorough comparison according to the observations from experiments in Section 7.

3 NETWORK CONTROL MODEL

In this section, we introduce a new HHWN control model, which considers real-world physical constraints. We first formulate a constrained optimization problem where the objective is to minimize the network communications energy (see Section 3.1). We then briefly describe a convex

model, which does not consider real-world physical constraints (see Section 3.2). Section 3.3 presents two nonconvex models: 1) a Morse potential force driven model involving power limitation constraints (maximum transmitted power at the network nodes); and 2) a new hybrid energy model that takes into account both power limitations as well as distance threshold constraints. It is worth pointing out that the convex model and the Morse potential force driven model were introduced in [12] and [2], respectively. The descriptions of these two models are included in this work for the sake of completeness.

3.1 Problem Statement

In HHWNs, a host s communicates with another host d by transmitting its information to the closest backbone node; then the traffic traverses the backbone network until it reaches the backbone node that is closest to the destination; and finally the backbone node that is closest to the destination transports the traffic to the host d . This scheme is based on two main properties: first, the end hosts need to be well covered by the backbone nodes, and second, the backbone nodes must have good connectivity among themselves [11]. Thus, network performance in HHWNs clearly depends on the joint optimization of network coverage and backbone connectivity.

Llorca et al. defined a cost function that takes into account the cost for network coverage and backbone connectivity, as the total communications energy stored in the wireless links forming the network, as follows [11], [12]:

$$U(b_{ij}, h_{ik}, B_1, B_2, \dots, B_N) = \alpha \cdot \sum_{i=1}^N \sum_{j=1}^N b_{ij} u(B_i, B_j) + \sum_{i=1}^N \sum_{k=1}^M h_{ik} u(B_i, T_k), \quad (5)$$

where B_i is the location of backbone node i , T_k is the location of terminal node k , N is the number of backbone nodes, M is the number of terminal nodes, α ($\alpha \geq 0$) is a weighting parameter to balance the energy used for forming the mesh backbone network and covering end hosts, b_{ij} and h_{ik} are the binary variables, which are given by

$$b_{ij} = \begin{cases} 1, & \text{if } (i, j) \in \Lambda_B \text{ is connected,} \\ 0, & \text{otherwise,} \end{cases} \quad (6)$$

where Λ_B refers to the backbone topology, and

$$h_{ik} = \begin{cases} 1, & \text{if } (i, k) \in \Lambda_T \text{ is connected,} \\ 0, & \text{otherwise,} \end{cases} \quad (7)$$

where Λ_T refers to the coverage topology, i.e., $h_{ik} = 1$ indicates that backbone node i covers terminal node k . The measurement of communication cost $u(B_i, B_j)$ is usually associated with the euclidean distance between link ends (i, j) and is precisely defined as the communications energy per unit time required to send information from node i and node j at the specified Bit Error Rate (BER) [3], [12]

$$u_{ij} = P_{R0}^j \frac{4\pi}{D_T^j A_R^j} (\exp(\gamma \|B_i - B_j\|)) (\|B_i - B_j\|^2), \quad (8)$$

where P_{R0}^j is the minimum received power, D_T^j is the directivity of the transmitter antenna, A_R^j represents the effective receiver area [37]. The scattering coefficient γ measures the attenuation electromagnetic radiation undergoes as it travels through the atmosphere due to the scattering effects caused by the presence of atmospheric agents in the form of suspended water particles such as fog, clouds, rain, or snow [2]. The calculation of $u(B_i, T_k)$ is similar to the calculation of $u(B_i, B_j)$. The end users always try to connect to the backbone node that is closest to them while satisfying physical constraints.

Note that the first term in the cost function in (5), denoted by U_{BB} , represents the total energy stored in the directional wireless links forming the mesh backbone network, and the second term in (5), denoted by U_{BT} , represents the total energy stored in the wireless links covering the end hosts. Thus, U_{BB} measures the cost for the backbone connectivity, i.e., a higher value of U_{BB} indicates a backbone topology that requires higher communications energy in order to maintain the connectivity of backbone nodes. On the other hand, a higher value of U_{BT} indicates a higher demand for communications energy in order to retain end hosts covered at the specified BER [2].

The topology control problem in HHWNs is then formulated as an energy minimization problem of the following form:

$$\min\{U(b_{ij}, h_{ik}, B_1, B_2, \dots, B_N)\} (B_i = (x_i^b, y_i^b, z_i^b), B_i \in R^3), \quad (9)$$

which is subject to (6) and (7). Note that the optimization problem formulated in (9) is performed over: b_{ij} , the assignment of directional wireless links between backbone nodes; h_{ik} , the assignment of wireless links between backbone nodes and covered end users; (B_1, B_2, \dots, B_N) , the location of the N backbone nodes. But the link assignments b_{ij} and h_{ik} , and the location of backbone nodes (B_1, B_2, \dots, B_N) must be subject to real-world physical constraints, which include:

- **Power limitation.** "Power limitation" refers to the maximum power at a transmitter. In practice, the increase in transmitted power needed to maintain a given link BER is limited by the maximum power at the transmitter. Both backbone nodes and terminal nodes have power limitations because either of them might be a transmitter or a receiver.
- **Traffic capacity.** "Traffic capacity" refers to the maximum traffic that a backbone node can receive and transfer. In this paper, the capacity of a backbone node is defined as the maximum number of terminal nodes a base station can handle.
- **Distance threshold.** "Distance threshold" is defined as the minimum distance for a backbone node to avoid collisions with another backbone node or a terminal node.
- **Taboo areas.** "Taboo areas" refers to constraints imposed by the physical world such as geographic obstacles (e.g., mountains and high-rise buildings), undesired weather events (e.g., heavy clouds or regions of precipitation), and security areas (e.g., signals are fully blocked because of security

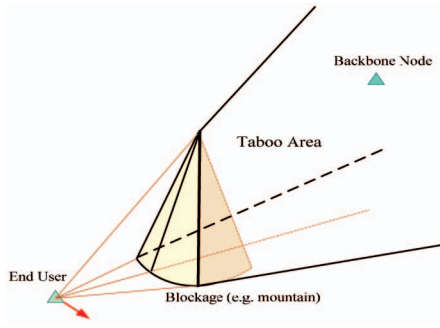


Fig. 2. An example of taboo area.

requirements, or jamming). It is worth noting that these taboo areas are dynamic. An example of a taboo area is illustrated in Fig. 2. Note that the taboo area (depicted as a cone delineated by a black line), for a particular backbone node changes dynamically with the movement of the end user (here, we assume total blockage if there is no direct line of sight between end user and backbone node; in fact, the signal attenuation due to blockage can be incorporated into the link energy function in (8)).

Let Θ represent the set of physical constraints, which includes power limitation C_p , traffic capacity of backbone nodes C_c , minimum physical distance C_d , and taboo areas C_t , i.e., $\Theta = \{C_p, C_c, C_d, C_t\}$, then the optimization problem described in (9) is transformed into

$$\begin{aligned} \min \{ & U(b_{ij}, h_{ik}, B_1, B_2, \dots, B_N) \} \\ \text{s.t. } & \Theta = \{C_p, C_c, C_d, C_t\}. \end{aligned} \quad (10)$$

3.2 Convex Model

Without taking into account the physical constraints Θ , Llorca et al. [3], [11], [12] introduced an iterative approach to solve the optimization problem described in (9). They reported that when assuming no physical constraints this is a convex problem, which can be solved by using gradient descent-based methods. In [3], [11], and [12], a force-based algorithm is used to dynamically relocate the backbone nodes in order to jointly optimize coverage and connectivity. At each step, the net force acting on backbone node i is computed as the negative energy gradient with respect to its location B_i , as follows:

$$\begin{aligned} F_i = -\nabla^i U = & \alpha \sum_{j=1}^N \delta(b_{ij} = 1) (-\nabla^i u_{ij}) \\ & + \sum_{k=1}^M \delta(h_{ik} = 1) (-\nabla^i u_{ik}), \end{aligned} \quad (11)$$

where $\delta(\cdot)$ is the indicator function (its value is 1 if the statement within its argument is true, and 0 otherwise) and $-\nabla^i u_i$ is the link energy gradient, which determines the force acting on backbone node i due to its interaction with neighbor node j , as follows:

$$f_i = -\nabla^i u_i = \left[-\frac{\partial u_i}{\partial x_i^a} - \frac{\partial u_i}{\partial y_i^b} - \frac{\partial u_i}{\partial z_i^c} \right]^T. \quad (12)$$

Thus, the location B_i of backbone node i at current iteration t is updated according to the following:

$$B_i(t+1) = B_i(t) + \rho \cdot F_i, \quad (13)$$

where ρ is the step size to allow the location change at every iteration. Then, the location of backbone nodes (B_1, B_2, \dots, B_N) is updated until the location change $\|B_i(t) - B_i(t-1)\|$ reaches the predefined resolution or the maximum number of iterations is reached. In this paper, we refer to this algorithm as the Attraction Force Driven algorithm (AFD).

3.3 Nonconvex Model

When taking into account the set of physical constraints Θ , the energy function U becomes nonderivative, which makes the problem a nonconvex problem. In order to address the constraints associated with power limitations at the network nodes, recently Llorca et al. [2] further extended the convex link energy function into a nonconvex function employing the Morse potential [13], which is used in molecular dynamics to characterize the potential energy stored in bonds within molecules. Using the Morse potential, the link energy function becomes

$$u_{il} = D_{il}(1 - \exp(-\tau_{il}\|B_i - T_l\|))^2, \quad (14)$$

where D_{il} is the ‘‘dissociation energy’’ and τ_{il} relates to directivity and other communication parameters of the wireless link (i, l) [2]. Thus, the force magnitude f_{il} acting on backbone node i from neighbor node l is given by [2]

$$f_{il} = 2D_{il}\tau_{il}(\exp(-\tau_{il}\|B_i - T_l\|) - \exp(-2\tau_{il}\|B_i - T_l\|)). \quad (15)$$

This nonconvex force model is used in [2] to develop an adaptive control strategy, where communication links are retained or released based on their cost in the network. As opposed to the AFD algorithm derived from the convex model, where links are always retained (as the force increases with distance) [11], [12], the adaptive algorithm developed in [2] allows the release of connections when the distance, or more precisely communications cost is too high. We refer to this algorithm as the Morse Force Driven (MFD) algorithm, which shows a significant improvement in the average number of Source-to-Destinations (SD) maintained, as compared to AFD [2].

In this research, we introduce a new continuous energy function that considers power limitations as well as distance threshold constraints, as an extension to the Morse energy model [13]. The basic idea with respect to considering a distance threshold between a backbone node and a terminal node (or another backbone node) is that the network nodes should repel each other when the distance between them decreases to a certain point. Let f_{il} be the force that the terminal node (or another backbone node) l exerts on backbone node i , the direction and magnitude of force f_{ik} is given by

$$f_{ik} = q(B_i - T_k), \quad (16)$$

where $q(\cdot)$ denotes the function of repulsion, retention, and release between the nodes. The repulsion/retention/release function we consider here is

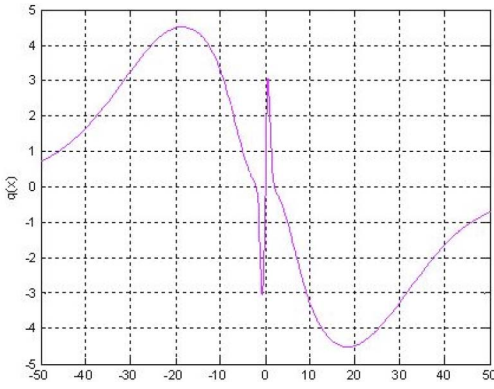


Fig. 3. Repulsion/retention/release function for one dimension.

$$q(x) = -x(a - b(\exp(-\|x\|^2/c)) + r(\exp(-\xi\|x\|^2) - \exp(-v\|x\|^2))), \quad (17)$$

where a , b , c , r , ξ , and v are positive constants such that $a < b$ and $\xi < v$. For the case with $x \in \mathbb{R}^1$, and $a = 0.005$, $b = 8$, $c = 0.8$, $r = 0.002$, $\xi = 0.0015$, and $v = 0.03$, the function is shown in Fig. 3. Note that when the link distance is smaller than 2, the repulsion force is the one acting on the nodes, while the release force acts after the distance increases to around 18. Note that the parameter a represents the retention to maintain the connection, the item $b(\exp(-\|x\|^2/c))$ represents the repulsion motivated by [38] for small distances, and the item $r(\exp(-\xi\|x\|^2) - \exp(-v\|x\|^2))$ represents the release of a connection [2] for long distances. We clarify that this hybrid function we introduce here overcomes the shortcomings of the attraction/repulsion function [38] that assumes an infinite sensing range, which is inconsistent with the real-world interactions among individuals. We believe that this hybrid function will provide insights for the stability analysis of HHWNs. These energy-based models, while leading to efficient, scalable, and physically accurate control methods for self-organization in HHWNs [2], [11], [12], they are parameter sensitive and require knowledge of the dynamics of the channel as well as explicit formulations of the energy functions, which can be difficult to obtain when considering dynamic taboo areas such as atmospheric agents and terrain. Furthermore, the presence of taboo areas makes gradient-based methods unable to guarantee convergence to globally optimal solutions.

Therefore, in this research, we propose to use two novel approaches for the self-organization and optimization of HHWNs, which do not require explicit knowledge of the channel nor rely on gradient methods: FA, which uses local information for system self-organization, and PSO, which needs global information for system optimization. We will investigate their performance in the context of HHWNs.

4 FLOCKING ALGORITHM

Recall that the objective in HHWNs is to optimize the total energy cost of the system while guaranteeing end-to-end communications with physical constraints. The problem has been transformed to relocate the positions of backbone nodes (see Section 3.1). We indicate that the use of energy functions (harmonic function, Morse function, and hybrid

function) makes it challenging to obtain the objective when taking into account all kinds of physical constraints that we include in this research. In this section, we develop a new FA using heuristic forces to model straightforwardly the effects of various constraints on the system.

4.1 Flocking Rules

In our model, each backbone node represents an agent in a flock. A terminal node $T_k(s)$ is assumed to be stationary during the movement of backbone nodes because of a time delay, which is consistent with practical situations. Here, s represents the time series of the terminal node dynamics. Thus, time $t \in [0, t_{\max}]$ (t_{\max} is the stopping time point) with respect to backbone nodes is a subinterval of $[s - 1, s]$ with respect to terminal nodes. A backbone node i at time t is characterized by its location $B_i(t)$ associated with the real coordinates $(x_i^b(t), y_i^b(t), z_i^b(t))$ and its force vector (or velocity vector) $v_i(t)$. Let $b_{ij}(t)$ and $h_{ik}(t)$ be the link assignment variables for backbone-to-backbone links and backbone-to-terminal links at time t , respectively. The forces acting on backbone node i include:

- **Survival force.** The “survival force” makes a backbone node try to maintain connection to those terminal nodes it had covered at the last time period $s - 1$. This force enables the effective reduction in the loss of the closest terminal nodes to backbone node i due to the existence of taboo areas such as geographic constraints. The force is given by

$$v_{agn}^i = \frac{\sum_k^M \delta(h_{ik}(s-1) = 1)(T_k(s-1) - B_i(t))}{\sum_k^M \delta(h_{ik}(s-1) = 1)}, \quad (18)$$

where $\delta(\cdot)$ is the indicator function (its value is 1 if the statement within its argument is true, and 0 otherwise).

- **Repulsion force.** The “repulsion force” is produced by three sources: terminal nodes covered by the backbone node i at the bottom layer in HHWNs, neighbor backbone nodes connected to backbone node i at the upper layer, and the terrain. The whole repulsion force is determined by

$$v_{pul}^i = v_{pul}^{i,BT} + v_{pul}^{i,BB} + v_{pul}^{i,ter}, \quad (19)$$

$$v_{pul}^{i,BT} = -\frac{\sum_k^M \delta(H_{sta})\delta(D_{sta}^{pul,BT})(T_k(s) - B_i(t))}{\sum_k^M \delta(H_{sta})\delta(D_{sta}^{pul,BT})}, \quad (20)$$

$$v_{pul}^{i,BB} = -\frac{\sum_j^N \delta(b_{sta})\delta(D_{sta}^{pul,BB})(B_j(t) - B_i(t))}{\sum_j^N \delta(b_{sta})\delta(D_{sta}^{pul,BB})}, \quad (21)$$

$$v_{pul}^{i,ter} = \delta(Z_{sta})((0, 0, z_i^{b,pro}(t)) - B_i(t)), \quad (22)$$

where, H_{sta} denotes the statement $(h_{ik}(t) = 1)$, $D_{sta}^{pul,BT}$ denotes the statement $(d_{BT}(T_k(s), B_i(t)) \leq d_{th,pul}^{BT})$, b_{sta} denotes the statement $(b_{ij}(t) = 1)$, $D_{sta}^{pul,BB}$ denotes the statement $(d_{BB}(B_j(t), B_i(t)) \leq d_{th}^{BB})$, Z_{sta} denotes the statement $(z_i^b(t) - z_i^{b,pro}(t) \leq d_{th}^{ter})$, $d_B(\cdot) = \|\cdot\|$ is a distance function, $d_{th,pul}^{BT}$ is the distance threshold

between backbone nodes and terminal nodes, d_{th}^{BB} is the distance threshold between backbone nodes, d_{th}^{ter} is the minimum distance between a backbone node and the ground, which is measured by the height difference in the z coordinate, i.e., $z_i^b(t) - z_i^{b,pro}(t)$. Note that the exerted repulsion force $v_{pul}^{i,ter}$ avoids collision with mountains or other obstacles on the ground. The repulsion force also contributes to the balance between network coverage and backbone connectivity and reduces the risk of solutions getting stuck in local minima, which can be observed from the experiments presented in Section 6.3.

- **Retention force.** The “retention force” is produced by two sources and it is calculated according to

$$v_{ten}^i = v_{ten}^{i,BT} + v_{ten}^{i,BB}, \quad (23)$$

$$v_{ten}^{i,BT} = \frac{\sum_k^M \delta(H_{sta}) \delta(D_{sta}^{ten,BT})(T_k(s) - B_i(t))}{\sum_k^M \delta(H_{sta}) \delta(D_{sta}^{ten,BT})}, \quad (24)$$

$$v_{ten}^{i,BB} = \frac{\sum_j^N \kappa_{ij} \delta(b_{sta}) \delta(D_{sta}^{ten,BB})(B_j(t) - B_i(t))}{\sum_j^N \delta(b_{sta}) \delta(D_{sta}^{ten,BB})}, \quad (25)$$

where, $D_{sta}^{ten,BT}$ denotes the statement ($d_{th,pul}^{BT} \leq d_{BT}(T_k(s), B_i(t)) \leq d_{th,lea}^{BT}$), $D_{sta}^{ten,BB}$ denotes the statement ($d_{th}^{BB} \leq d_{BB}(B_j(t), B_i(t))$), $d_{th,lea}^{BT}$ is another distance threshold between backbone nodes and terminal nodes (we explain it in the following section), and κ_{ij} is a coefficient that considers the effect of sharing the load between backbone nodes, which is defined by

$$\kappa_{ij} = \exp\left(\frac{R_j - \sum_k^M \delta(H_{sta}) + \sum_k^M \delta(H_{sta})}{R_j}\right), \quad (26)$$

where R_j is the capacity of the backbone node j .

- **Release force.** The “release force” is used to consider the effect of power limitation, which is controlled by a distance threshold $d_{th,lea}^{BT}$. Here, we only consider the release force between backbone nodes and terminal nodes because a large power between backbone nodes is usually available in practice to assure the connectivity at the upper layer. The release force is given by

$$v_{lea}^i = \frac{\sum_{k=1}^M \gamma_{ik} \delta(H_{sta}) \delta(D_{sta}^{lea,BT})(T_k(s) - B_i(t))}{\delta(H_{sta}) \delta(D_{sta}^{lea,BT})}, \quad (27)$$

where, $D_{sta}^{lea,BT}$ denotes the statement ($d_{th,lea}^{BT} \leq d_{BT}(T_k(s), B_i(t))$), and γ_{ik} is a release coefficient determined by

$$\gamma_{ik} = \exp(-\varepsilon(d_{BT}(T_k(s), B_i(t)) - d_{th,lea}^{BT})), \quad (28)$$

in which ε is a positive constant with small value, in this paper we set $\varepsilon = 0.001$.

In order to achieve comprehensive flocking behavior, we sum up all the forces described above to obtain a net velocity for the backbone node i as follows:

$$v_i(t) = v_{ten}^i(t) + w_p v_{pul}^i(t) + w_l v_{lea}^i(t) + w_a v_{agn}^i(t), \quad (29)$$

where w_p , w_l , and w_a are positive weighting parameters to balance the effects of the different forces. Then, the location of backbone node i is updated according to the following:

$$B_i(t+1) = B_i(t) + \rho \cdot v_i(t). \quad (30)$$

Based on this flocking model, we are capable of straightforwardly addressing constraints such as power limitation with the use of the release force v_{lea}^i , capacity with the use of the sharing function κ_{ij} , distance threshold with the use of the repulsion force v_{pul}^i , and taboo areas with the use of the survival force.

4.2 Algorithm and Implementation

Our FA algorithm is developed using the above flocking rules and based on discrete time events. Suppose all the terminal nodes update their positions synchronously at every time interval $[s, s+1]$ (e.g., every minute), and all the backbone nodes move synchronously to update their positions and velocities at every time step t until the movement of each backbone node is smaller than a predefined resolution μ , i.e., $\|B_i(t) - B_i(t-1)\| \leq \mu$, or the maximum number of iterations t_{max} is satisfied. Given a new input of coordinates of all the terminal nodes $\{T_k(s)\}$ ($k = 1, 2, \dots, M$), and the initial locations (i.e., the old locations at last time interval) of the backbone nodes $\{B_i(0)\}$ ($i, j = 1, 2, \dots, N$), we first calculate the coverage topology $h_{ik}(0)$ ($i = 1, 2, \dots, N; k = 1, 2, \dots, M$) while satisfying physical constraints. In the current implementation, the constraints with respect to taboo areas only include mountains in a 3D space with full terrain information. A large number of mountains with different heights are randomly generated. In the simulation environment, we partition the x - y plane with a fixed grid size, which is fine enough to produce satisfactory resolution, corresponding to a terrain matrix $A_{terrain} = [a_{pq}]_{m \times m}$, where each component represents the altitude of a point in the x - y plane. Given a terminal node with location $T_k = (x_k^t, y_k^t, z_k^t)$ and a backbone node locating at $B_i = (x_i^b, y_i^b, z_i^b)$, we have developed an effective approximation algorithm to evaluate if there is direct line of sight between the terminal node T_k and the backbone node B_i bearing in mind the location of mountains. In this research, we only consider blockage between terminal nodes and backbone nodes, as the backbone nodes are usually located at fixed high altitudes. It is easy to extend our approach to include blockage between backbone nodes in military applications. The terrain checking algorithm is aided by the interpolation function “interp1” from the MATLAB toolbox (we used MATLAB as our simulation environment).

Forming the coverage topology, we first check the constraints from the terrain. The basic idea is that each terminal node will first connect to its closest backbone node. If there is no line of sight between them, we put the backbone node into a taboo archive and connect to the second closest backbone node. The process stops when a connection is achieved that satisfies the geographic constraints. If there is no line of sight for all the backbone nodes, the terminal node is considered isolated. We then consider the capacity constraint R_i ($i = (1, 2, \dots, N)$), i.e., the maximum number of terminals that can be connected to each backbone node. In other words, if the number of terminals n_i connecting to

backbone node i exceeds the capacity R_i , we reconnect $(n_i - R_i)$ terminals to other backbone nodes. The selection of terminal nodes that need to be reconnected is based on the minimum-energy-cost-first principle. The capacity checking process is similar to the geography checking algorithm, but the reconnection to other backbone nodes is required to first satisfy the geographic algorithm, i.e., the geography checking algorithm is embedded in this process. Finally, the overall implementation for the flocking algorithm is summarized as follows:

1. Given the initial positions of terminal nodes $\{T_k(0)\}$, the physical constraints $\Theta = \{C_p, C_c, C_d, C_t\}$, set time $s = 0$ for the dynamics of terminal nodes.
2. Given the initial positions of backbone nodes $\{B_i(0)\}$, set time $t = 0$ for the dynamics of backbone nodes.
3. Set time $t \leftarrow t + 1$, use the topology configuration algorithm [39] to determine $\{b_{ij}\}$, then check the geographic constraints and the capacity constraints for all the terminal nodes to determine the coverage topology $\{h_{ik}\}$.
4. Calculate the force or velocity $v_i(t)$ for the backbone node i according to (29).
5. Update the positions of backbone nodes $\{B_i(t)\}$ according to (30).
6. Evaluate $\|B_i(t) - B_i(t-1)\|$ for each backbone node, if $\|B_i(t) - B_i(t-1)\| \leq \mu$, then fix the current position of backbone node i . If the maximum number of iterations t_{\max} is satisfied, go to Step 7; otherwise, go to Step 3.
7. Set time $s \leftarrow s + 1$, terminal nodes move to new positions $\{T_k(s)\}$, i.e., the new dynamics from terminal nodes. Set $B_i(0) \leftarrow B_i(t)$ for each backbone node, and go to Step 2 until simulation is over.

Note that the FA can be executed in a distributed manner because each backbone node only uses local information from neighbor backbone nodes and the terminal nodes in its coverage range. It is difficult to provide an explicit form with respect to the computational time complexity of the whole system because of the heterogeneous dynamics of the end users. In each time step t , the computational time complexity approximates to $O(NM)$, where we do not take into account the computation time required for the geography and capacity checking algorithms. In practice, geographic information can be directly obtained by the system almost in real time. The computational time with respect to the capacity checking algorithm is closely related to the dynamics of the end users and backbone nodes.

5 PARTICLE SWARM OPTIMIZER

As described in Section 3, the topology control problem in HHWNs can be effectively formulated as an energy minimization problem whose solution jointly optimizes coverage and connectivity in dynamic environments. We have developed a new FA described in the last section using local information to control the system such that the HHWN is autonomously self-organized. In this section, we use PSO, a stochastic global optimization algorithm, to investigate the performance of using global information

from the entire system for the optimization of HHWNs. The use of global information is expected to produce better solutions at the expense of longer convergence time and scalability limitations. The performance of PSO will also be useful to evaluate and compare the performance of distributed algorithms such as AFD [11], MFD [2], and FA. In this section, we develop the encoding scheme, evaluation function, and implementation issues for PSO within the optimization framework for HHWNs.

5.1 Encoding and Evaluation Function

In PSO, each particle represents a solution to the problem. In HHWNs, the solution is the location of the backbone nodes (B_1, B_2, \dots, B_N) that minimizes the total energy of the system while satisfying real-world physical constraints. We use a stack vector to encode particle l as $X_l = (x_{l,1}, x_{l,2}, \dots, x_{l,d})$ in the following way:

$$\begin{aligned} X_l &= (x_{l,1}, x_{l,2}, \dots, x_{l,d}) \\ &= \left(\underbrace{(x_1^b, y_1^b, z_1^b)}_{B_1}, \underbrace{(x_2^b, y_2^b, z_2^b)}_{B_2}, \dots, \underbrace{(x_i^b, y_i^b, z_i^b)}_{B_i}, \dots, \underbrace{(x_N^b, y_N^b, z_N^b)}_{B_N} \right), \end{aligned} \quad (31)$$

where $d = 3N$ is the dimension size that each particle explores in this optimization problem.

One important aspect of this optimization process is to design effectively an evaluation function that characterizes the network's energy cost while taking into account the physical constraints. We define a comprehensive evaluation function

$$\begin{aligned} f &= \underbrace{\sum_{i=1}^N \sum_{k=1}^M h_{ik} u(B_i, T_k)}_{U_{BT}} \\ &+ \alpha \cdot \underbrace{\sum_{i=1}^N \sum_{j=1}^N b_{ij} u(B_i, B_j)}_{U_{BB}} \\ &+ \beta \cdot \underbrace{\sqrt{\left(\sum_{i=1}^N \left(\sum_{k=1}^M h_{ik} - \bar{E} \right)^2 \right)}}_{U_{STD}} / N \\ &+ \lambda \cdot \underbrace{\left(M - \sum_{i=1}^N \sum_{k=1}^M h_{ik} \right)}_{U_{LOS}}, \end{aligned} \quad (32)$$

where $\bar{E} = \sum_{i=1}^N \sum_{k=1}^M h_{ik} / N$ is the average number of terminal nodes connected to a backbone node. The first term U_{BT} is the total energy cost for network coverage as described in (5) and the second term U_{BB} is the total energy cost for backbone connectivity. The third term U_{STD} is the standard deviation of the number of terminal nodes connected to a backbone node which characterizes the distribution of backbone-to-terminal connections per backbone node. This term is used to make backbone nodes share the end-users' loads. Finally, the term U_{LOS} is the number of lost connections or number of terminals not connected to any backbone node. α ($\alpha \geq 0$) and β ($\beta \geq 0$) are weighting parameters, whereas parameter λ is a large number used to increase the weight on the Loss of Connections (LC) cost (in this research, we set it at $\lambda = 10^6$). Note that this function

includes the effects of backbone connectivity, backbone coverage, connection distribution, and loss of connections on the system, which drives the system's self-organization and optimization in a comprehensive manner.

5.2 Implementation

Based on the above encoding scheme and evaluation function, we develop a PSO algorithm for the optimization of HHWNs. In the initialization process, the particles are clamped into the following space:

$$Q = [x_1^b(0) \pm r_{\max}, y_1^b(0) \pm r_{\max}, z_1^b(0) \pm r_{\max}, \dots, x_N^b(0) \pm r_{\max}, y_N^b(0) \pm r_{\max}, z_N^b(0) \pm r_{\max}], \quad (33)$$

where r_{\max} represents the distance that a backbone node can move from the initial position at time $t = 0$ for the time interval $[s - 1, s]$. In the evolution process, each particle is constrained to a finite space where all the terminal nodes move. In the simulation environment, the space is usually a cube, i.e., $\{x_i^b, y_i^b, z_i^b\} \in [v_{\min}, v_{\max}]$. Thus, each element in $X_l = (x_{l,1}, x_{l,2}, \dots, x_{l,d})$ is in the range of $[v_{\min}, v_{\max}]$. Similar to the use of FA, we use PSO in every time interval $[s - 1, s]$ and optimize the location of backbone nodes (B_1, B_2, \dots, B_N) until the maximum number of iterations t_{\max} is met. During the evaluation of the optimality of each particle, we first use the approximation algorithm [39] to perform the backbone topology reconfiguration, and then check the geographic constraints and the capacity constraints for all the terminal nodes to determine the coverage topology for the current location of backbone nodes. The overall optimization procedure using PSO is summarized as follows:

1. Given the initial positions of terminal nodes $\{T_k(0)\}$, the physical constraints $\Theta = \{C_p, C_c, C_d, C_t\}$, set time $s = 0$ for the dynamics of terminal nodes.
2. Given the initial positions of backbone nodes $\{B_i(0)\}$, set time $t = 0$ for the dynamics of backbone nodes.
3. Initialize the positions of particles $X(t) = \{X_l(t)\}$ according to (33), set the initial velocities of particles $V(t) = X(t) = \{V_l(t)\}$.
4. Use the topology reconfiguration algorithm [39] to determine b_{ij} , then check the geographic constraints and the capacity constraints for all the terminal nodes to determine the coverage topology h_{ik} . Evaluate the fitness of particle $X_l(t)$ ($l = 1, 2, \dots, N_p$; N_p is the number of particles in the swarm).
5. Initialize the local best $P(t) = \{P_l(t)\}$ for each particle and the global best $G(t)$ for the whole swarm.
6. Set time $t \leftarrow t + 1$ and calculate inertia weight $w(t)$ according to (3).
7. Update the velocity $V(t) = \{V_l(t)\}$ and position $X(t) = \{X_l(t)\}$ according to (2) and (4), respectively.
8. Use the topology reconfiguration algorithm [39] to determine b_{ij} , then check the geographic constraints and the capacity constraints for all the terminal nodes to determine coverage topology h_{ik} . Evaluate the fitness of particle $X_l(t)$ ($l = 1, 2, \dots, N_p$).
9. Update the local best $P(t) = \{P_l(t)\}$ for each particle and the global best $G(t)$ for the whole swarm.
10. If the maximum number of iterations t_{\max} is satisfied, go to Step 11; otherwise, go to Step 6.

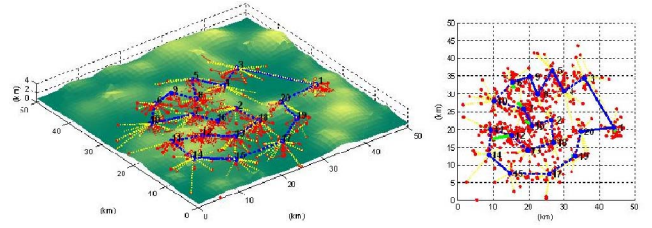


Fig. 4. An example of a dynamic scenario.

11. Set time $s \leftarrow s + 1$, terminal nodes move to new positions $\{T_k(s)\}$, i.e., the new dynamics from terminal nodes. Set $B_i(0) \leftarrow B_i(t)$ for each backbone node, and go to Step 2 until simulation is over.

Note that PSO uses global information from all the backbone nodes to evaluate the optimum placement of each particle and then selects the global best as the best possible solution to the system when the maximum number of iterations is met. The computational time complexity of PSO at every time step t approximates $O(N_p \times (3N + NM))$, which relies on the number of particles in the swarm and the number of backbone nodes, without taking into account the computational time from the geography and capacity checking algorithms.

6 EXPERIMENTS

6.1 Experimental Setup

In order to verify the performance of our proposed self-organization and optimization algorithms for HHWNs, we conducted extensive experimental studies and present the corresponding results for different dynamic scenarios and design parameters. In all simulations, M terminal nodes are distributed over a 50 km \times 50 km plane and organized in clusters using the Minimum Spanning Tree algorithm [40]. N_m mountains are randomly generated in this plane with a maximum height of 1.6 km (we set $N_m = 80$ in this research). The altitudes of terminal nodes are updated according to the terrain. The backbone network in the upper layer is constructed using N backbone nodes forming a ring topology. We use ring topologies for the backbone network to assure resilience through bi-connectivity. An example running in this simulation platform is shown in Fig. 4, where $M = 500$, $N = 20$, small red dots represent terminal nodes and large blue dots represent backbone nodes. Terminal nodes move according to the RPGM model [41]. We place the backbone nodes at an altitude of 2 km, which indicates the backbone nodes move in 2D space (i.e., x - y plane), and compare FA and PSO to the Attraction Force Driven model [11] and the Morse Force Driven model [2]. FA, PSO, AFD, and MFD are used to make backbone nodes adjust their locations until convergence to the best possible backbone configuration.

In our experiments, FSO links with 2 mrad half beam divergence [42] are used for the backbone-to-backbone links and RF links with $\pi/4$ rad half beam divergence for the backbone-to-terminal links. The minimum required received power used was -45 dBm (31.6 nW) for all network nodes. The scattering coefficient γ is set to zero. We set the power limitation for both backbone nodes and terminal

TABLE 4
Performance of Average Energy Cost for Scenario I

Algorithm	Initial	Optimized	Energy Save
FA	836.95	572.31	31.62%
PSO	817.24	530.31	35.11%
MFD	1034.20	857.84	17.05%
AFD	881.10	640.57	27.30%

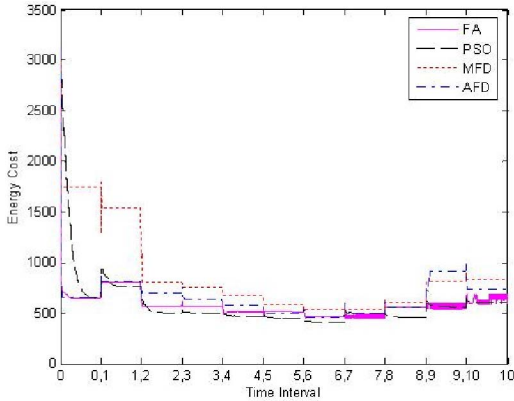


Fig. 5. Evolution of energy cost against time interval for scenario I.

TABLE 5
Comparative Results of Source-to-Destination Connections for Scenario I

Time	0	1	2	3	4	5	6	7	8	9	10	
FA	Initial	1122	3080	2352	3306	3422	4556	4032	4290	4032	3906	3782
	Optimized	3442	3660	4160	4160	4556	4422	4556	5122	4692	4422	4556
PSO	Initial	1122	3660	3906	4290	4032	3540	4830	5550	6006	5402	4692
	Optimized	3782	4160	5256	5112	4970	5550	5700	5256	6162	5550	4970
MFD	Initial	1122	1560	3660	4160	4160	4830	5112	5852	5550	4556	4970
	Optimized	2652	4032	4160	4422	4692	5256	5402	5550	5256	4970	5112
AFD	Initial	1122	3422	3422	3422	3306	3782	3906	4290	4160	3906	3906
	Optimized	3660	3660	3540	3540	4160	4556	4692	4970	4422	4290	3906

that FA delivers better results compared to AFD and MFD in overall simulation time. PSO achieves a significant improvement in energy cost while producing satisfactory results for LC. It is also noted that the energy cost produced by MFD decreases rather slowly during the first 4 minutes. That is because in MFD, long distance links are characterized by small forces (related to the release of connections), which makes the convergence to the initial optimal configuration slower than with the other algorithms. That is why after the same number of iterations, even AFD is able to obtain a better initial solution than that obtained by MFD. Table 4 shows the average energy cost for different algorithms according to Table 2. FA and PSO save 31.62 and 35.11 percent energy, respectively, which outperforms AFD and MFD. Fig. 5 visually illustrates the evolution of the energy cost corresponding to Table 2. It is observed that the convergence speed of FA, AFD, and MFD is faster than PSO but at the expense of getting stuck in local minima. Another observation is that the value of the energy cost produced by FA during minutes 4, 7, 9, and 10 oscillates, which is caused by the predefined resolution μ . In terms of the SD metric, we compare the results in Table 5 for every time interval and also summarize the average SD connections in Table 6. At minute 8, PSO achieves 6162 SD connections, which is much better than other methods.

TABLE 6
Performance of Average Source-to-Destination Connections for Scenario I

Algorithm	Initial	Optimized	Energy Save
FA	3443.6	4340.7	26.05%
PSO	4275.5	5133.5	20.07%
MFD	4139.3	4682.2	13.12%
AFD	3513.1	4126.9	17.47%

TABLE 7
Comparative Results of Energy Cost for Scenario II

Time	0	1	2	3	4	5	6	7	8	9	10	
FA	Initial	19910.0	2834.1	2662.9	2628.4	2879.5	3058.1	2778.4	2723.2	2751.3	2710.0	2700.6
	Optimized	2597.9	2881.1	2446.0	2465.4	2725.9	2720.7	2534.7	2666.0	2637.8	2507.3	2714.7
PSO	Initial	19910.0	3468.4	2691.0	2587.0	2660.5	3044.2	2718.0	2635.6	2682.9	2571.1	2735.1
	Optimized	2916.0	2549.3	2391.6	2397.7	2486.3	2563.2	2476.3	2446.2	2406.9	2414.5	2489.4
MFD	Initial	19910.0	2932.7	2958.3	2648.4	2898.4	3099.4	2824.5	3047.7	2764.6	2843.1	2884.0
	Optimized	3169.5	2717.0	2978.6	2527.1	2666.9	2853.8	2887.4	2758.6	2797.5	2683.2	2895.0
AFD	Initial	19910.0	2911.4	3014.6	2656.4	2668.4	3169.7	2833.0	2816.6	2721.1	2635.5	3056.7
	Optimized	3006.4	2618.7	2569.6	2523.2	2685.2	2891.6	2690.7	2676.1	2528.5	2638.4	2843.3

TABLE 8
Ratio of Lost Connections to Total Connections for Scenario II

Time	0	1	2	3	4	5	6	7	8	9	10	
FA	Initial	44/500	1/500	0/500	2/500	5/500	0/500	1/500	2/500	1/500	1/500	2/500
	Optimized	2/500	1/500	1/500	3/500	3/500	1/500	1/500	2/500	1/500	1/500	2/500
PSO	Initial	44/500	1/500	0/500	2/500	5/500	0/500	1/500	1/500	1/500	1/500	2/500
	Optimized	3/500	0/500	0/500	2/500	2/500	0/500	0/500	1/500	1/500	1/500	2/500
MFD	Initial	44/500	1/500	1/500	3/500	5/500	2/500	1/500	2/500	1/500	1/500	3/500
	Optimized	1/500	1/500	2/500	3/500	5/500	1/500	1/500	2/500	1/500	2/500	2/500
AFD	Initial	44/500	2/500	1/500	3/500	6/500	1/500	1/500	1/500	1/500	1/500	2/500
	Optimized	2/500	3/500	2/500	3/500	4/500	0/500	1/500	1/500	1/500	1/500	2/500

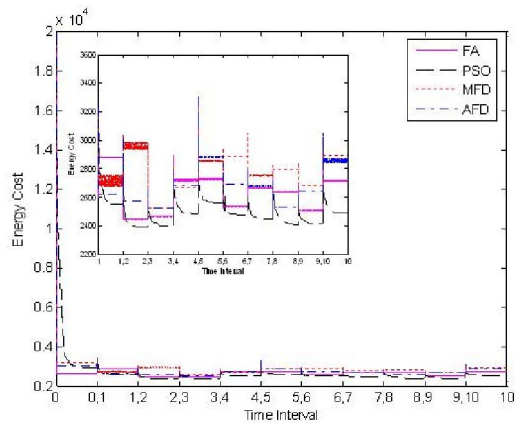


Fig. 6. Evolution of energy cost against time interval for scenario II.

From minute 3 to 7, MFD produces a larger number of SD connections than FA and AFD. But FA delivers a more significant improvement based on the average SD connections as shown in Table 6. It is noted that although MFD achieves a large number of average SD connections, the improvement it delivers is relatively small due to the large initial number of SD connections.

For scenario II, with 500 terminal nodes and 20 backbone nodes, the energy cost in each time interval and the total average cost are summarized in Tables 7 and 9. Table 8 shows the results associated with the LC metric. We observe that PSO consistently outperforms other methods, but its convergence speed is slower, as shown in Fig. 6. FA and PSO perform slightly better than MFD and AFD in

TABLE 9
Performance of Average Energy Cost for Scenario II

Algorithm	Initial	Optimized	Energy Save
FA	4330.6	2627.0	39.34%
PSO	4336.7	2503.4	42.27%
MFD	4437.4	2812.2	36.63%
AFD	4399.4	2697.4	38.69%

TABLE 10
Comparative Results of Source-to-Destination Connections for Scenario II

Time	0	1	2	3	4	5	6	7	8	9	10	
FA	Initial	4290	93942	90300	96410	83810	72092	81510	84390	89700	100172	102080
	Optimized	100172	114582	115260	105950	88506	83232	96410	99540	104652	115260	115940
PSO	Initial	4290	79242	90902	86142	89700	88506	86142	90902	89102	91506	95790
	Optimized	88506	102720	115940	106602	102080	106602	100806	102720	110556	109892	107256
MFD	Initial	4290	108570	105300	92720	85556	80372	83810	80940	97656	102080	100806
	Optimized	109892	122850	115940	107256	89102	95172	87912	97032	105300	114582	117306
AFD	Initial	4290	91506	100172	86142	83232	79242	79242	79806	92720	97656	98910
	Optimized	100172	113232	105300	98282	90902	91506	88506	98282	109892	105300	111890

TABLE 11
Performance of Average Source-to-Destination Connections for Scenario II

Algorithm	Initial	Optimized	Energy Save
FA	81700	103590	26.79%
PSO	81111	104880	29.30%
MFD	85645	105670	23.38%
AFD	81174	101210	19.80%

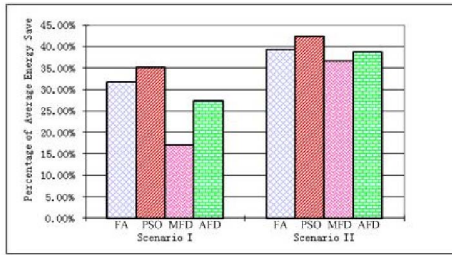


Fig. 7. Percentage of average energy saving for different scenarios.

terms of average energy saved as observed from Table 9. As shown in Table 10, MFD produces larger number of SD connections in the first three intervals compared to other methods. For overall time intervals, compared to the initial configuration of HHWN, 26.79 and 29.30 percent improvements of SD connections are achieved by FA and PSO as shown in Table 11.

In summary, we have listed the performance of the proposed FA and PSO algorithms in terms of energy savings and improvement in SD connections for different scales of HHWNs as shown in Figs. 7 and 8. We have also compared the results with the performance of existing AFD [11] and MFD [2] algorithms. It is observed that with an increase of the scale of the network the percentage of energy savings produced by FA, MFD, and AFD, increases, whereas the improvement in SD connections produced by PSO increases. From these comparative results, PSO performs best over all the scenarios, but its convergence speed is relatively slower, which is indicated by Figs. 5 and 6. FA delivers significantly good performance in terms of all the metrics and also exhibits a fast convergence speed. It is also observed that the solutions produced by FA, MFD, and AFD easily get stuck in local minima, which is caused by

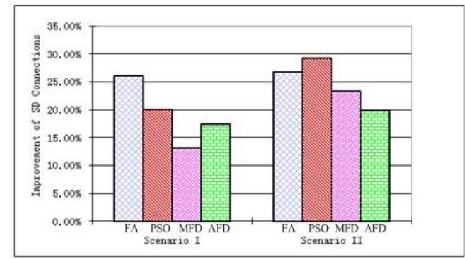


Fig. 8. Improvement of average SD connections for different scenarios.

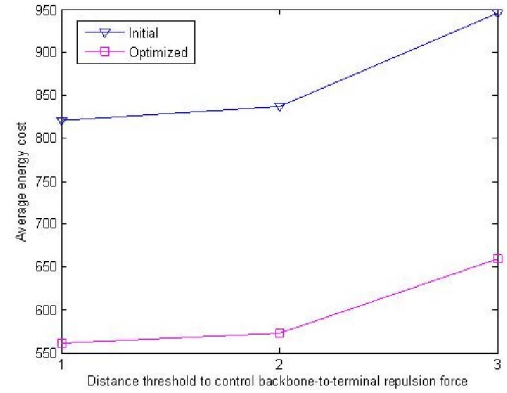


Fig. 9. Average energy cost versus distance threshold $d_{th,pul}^{BT}$.

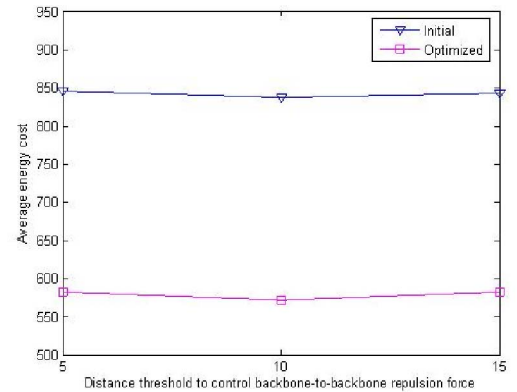


Fig. 10. Average energy cost versus distance threshold d_{th}^{BB} .

the existence of physical constraints (e.g., taboo areas) and the fact that they only use local information.

6.4 Parametric Study

In this section, we conduct an empirical study on the parameters involved in the FA model and their effects on the performance metrics. It includes the study of the distance threshold $d_{th,pul}^{BT}$ to control the backbone-to-terminal repulsion force, the distance threshold d_{th}^{BB} to control the backbone-to-backbone repulsion force, the distance threshold $d_{th,lea}^{BT}$ to control the backbone-to-terminal release force, and the resolution μ (see Section 4).

We use the average energy cost to measure the effects of these parameters. Scenario I, i.e., 100 terminal nodes and 10 backbone nodes, is used as the simulation platform. Fig. 9 shows the results of average energy cost against the distance threshold $d_{th,pul}^{BT}$ with respect to the initial configuration and the optimized HHWN structure. It indicates that the initial and optimized energy costs both increase with an increase of the distance threshold $d_{th,pul}^{BT}$, varying from 1 km to 3 km. However, as shown in Fig. 10,

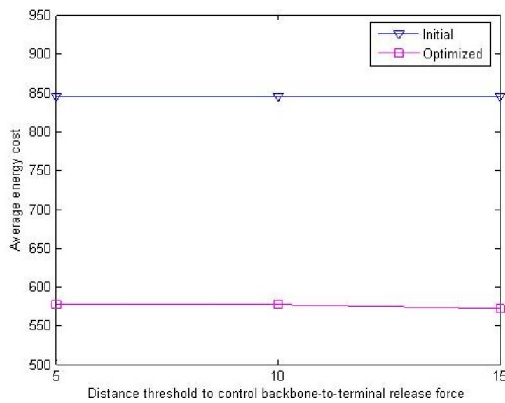


Fig. 11. Average energy cost versus distance threshold $d_{th,lea}^{BT}$.

increasing the distance threshold d_{th}^{BB} from 5 km to 15 km, which is used to control the backbone-to-backbone repulsion force, does not significantly affect the average energy cost. This phenomenon is caused by equally balancing the forces for backbone-to-backbone links and backbone-to-terminal links. It is easy to use a weighting coefficient to flexibly balance these two types of links. The effect of weighting coverage and connectivity costs on the total energy cost has been thoroughly analyzed in [11]. Changing the distance threshold $d_{th,lea}^{BT}$ to control the backbone-to-terminal release force also produces slight changes in the average energy cost as shown in Fig. 11, which is caused by FA favoring coverage cost such that every backbone node tightly follows the terminal nodes it covers while counteracting the release force. We use a predefined resolution μ to control the exploration of FA. The performance of setting the resolution μ at 0.01, 0.05, 0.1, and 0.5 is demonstrated in Fig. 12. For the case of $\mu = 0.1$, the performance is better in terms of producing lower energy cost. The choice of resolution μ depends on practical applications. On the other hand, we clarify that a smaller resolution makes FA need more computational time to converge to the best possible solution.

7 DISCUSSION

From the comparative results, we observe that PSO consistently delivers superior performance over FA, MFD, and AFD in terms of energy cost in an HHWN. We believe that this can be attributed to the use of global information and the stochastic property of PSO, which enables it to transcend local minima. On the other hand, FA also performs better compared to MFD and AFD, which is attributed to the use of heuristic forces, i.e., repulsion, retention, and release, instead of only considering the retention force by AFD [11] and the retention-release force by MFD [2]. We summarize the comparative features of FA and PSO in the following:

- FA uses local information with respect to every backbone node, whereas PSO needs global information of an HHWN to evaluate the whole performance of the system.
- The convergence speed of FA is much faster than PSO, but the solutions it produces are subject to local minima.

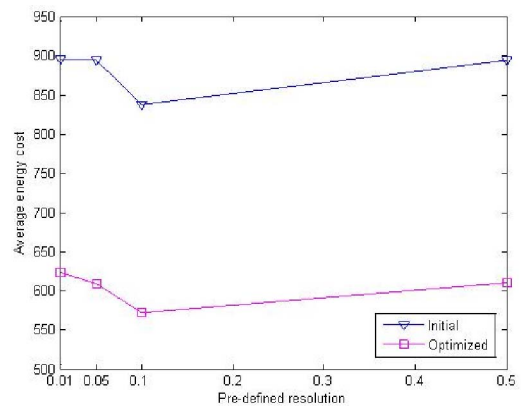


Fig. 12. Average energy cost versus resolution μ .

- FA can be implemented in a distributed way, whereas PSO supports parallel computing of the updates of solutions with the use of global information.
- Heuristic forces are used in FA to maintain the connectivity and coverage architecture of an HHWN, which can be transformed into an optimization problem, whereas PSO enables us to optimize the HHWN directly by defining a fitness function.
- PSO usually produces better solutions for more complex wireless communication environments, which is attributed to its stochastic global optimization strategy.
- With the use of FA, the backbone nodes are enabled to flexibly move in 3D space by taking into account the repulsion force from the physical constraints (e.g., mountains). On the contrary, it is difficult to use PSO in this case because the range in the z coordinate that particles roam in depends on the heights of mountains such that the exploration space becomes unsmooth.

It should be noted that we are not attempting to map real-world network scenarios into actual biological systems. The use of flocking rules and swarming behavior is generalizable and applicable to controlling and optimizing an HHWN. Actually, the flocking behavior of backbone nodes does not exactly map to that in biological systems. Based on the observations drawn from our experiments, we clarify that it is possible to develop a unified system using both FA and PSO algorithms, where the FA algorithm is used to control the HHWN in a distributed manner and provide initial solutions, while PSO can be used for finer system optimization, especially in complex environments, and when global information is available.

8 CONCLUSIONS AND FUTURE WORK

This paper presents new models and algorithms for control and optimization of a class of next generation communication networks: hierarchical heterogeneous wireless networks, under real-world physical constraints. An HHWN is characterized by directional wireless links connecting backbone nodes at the upper layer and dynamic terminal nodes at the bottom layer. First, we propose a mathematical modeling method for the self-organization and optimization

of HHWNs by taking into account physical constraints in terms of minimum distance threshold, power limitations, and capacity of backbone nodes. Second, using only local information, we develop new flocking rules and a corresponding algorithm to autonomously assure, control, and optimize network performance in a practical way. Associated physical constraints checking algorithms are also developed. Third, we use Particle Swarm Optimization, a stochastic global optimization algorithm, to optimize an HHWN directly with a hybrid evaluation function and using global information.

Experimental results confirm that our flocking algorithm and PSO both perform well for the optimization of an HHWN in terms of performance metrics such as energy cost, loss of connections, and number of SD connections. PSO produces superior performance but results in a relatively slow convergence speed and only favors the dynamics of backbone nodes in the x - y plane. FA is capable of delivering fast convergence speed while achieving satisfactory solutions for an HHWN. Furthermore, with the use of FA, the backbone nodes can move flexibly in 3D space by taking into account the repulsion force from the physical constraints (e.g., mountains). In future work, we plan to investigate our algorithms in more complex dynamic environments. We also note that the stability analysis of dynamic HHWNs is still an open problem, and we plan to conduct a theoretical analysis of the stability of an HHWN in the context of self-organization and control.

ACKNOWLEDGMENTS

The authors wish to thank Peter Pham for preparing the software development associated with the terrain checking algorithm and Professor Guanrong (Ron) Chen for his valuable suggestions and feedback with respect to this paper and related research. This research was supported in part by the US Air Force Office of Scientific Research under Contract No. FA95500910121 and the US National Science Foundation under Grant No. ECCS0946955.

REFERENCES

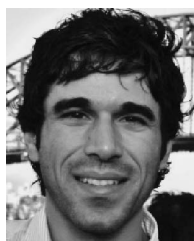
- [1] P. Gupta and P.R. Kumar, "The Capacity of Wireless Networks," *IEEE Trans. Information Theory*, vol. 46, no. 2, pp. 388-404, Mar. 2000.
- [2] J. Llorca, S.D. Milner, and C.C. Davis, "Molecular System Dynamics for Self-Organization in Heterogeneous Wireless Networks," *EURASIP J. Wireless Comm. and Networking*, in press, 2010.
- [3] S.D. Milner, J. Llorca, and C.C. Davis, "Autonomous, Reconfiguration and Control in Directional Mobile Ad Hoc Networks," *IEEE Circuits and Systems Magazine*, vol. 9, no. 2, pp. 10-26, Apr.-June 2009.
- [4] C.C. Davis, Z. Haas, and S. Milner, "On How to Circumvent the MANET Scalability Curse," *Proc. IEEE Military Comm. Conf. (MILCOM)*, 2006.
- [5] C.C. Davis, I.I. Smolyaninov, and S.D. Milner, "Flexible Optical Wireless Links and Networks," *IEEE Comm. Magazine*, vol. 41, no. 3, pp. 51-57, Mar. 2003.
- [6] S. Milner et al., "Self-Organizing Broadband Hybrid Wireless Networks," *J. Optical Networking*, vol. 4, pp. 446-459, 2005.
- [7] J. Llorca, A. Desai, S.D. Milner, and C.C. Davis, "Optimizing Performance of Hybrid FSO/RF Networks in Realistic Dynamic Scenarios," *Proc. SPIE Free Space Laser Comm. V*, vol. 5892, pp. 52-60, 2005.
- [8] C.K. Toh, *Ad Hoc Mobile Wireless Networks*. Prentice Hall, 2002.
- [9] J. Li et al., "Capacity of Ad Hoc Wireless Networks," *Proc. Seventh ACM Int'l Conf. Mobile Computing and Networking*, 2001.
- [10] B. An and S. Papavassiliou, "A Mobility-Based Clustering Approach to Support Mobility Management and Multicast Routing in Mobile Ad-Hoc Wireless Networks," *Int'l J. Network Management*, vol. 11, pp. 387-395, 2001.
- [11] J. Llorca, M. Kalantari, S.D. Milner, and C.C. Davis, "A Quadratic Optimization Method for Connectivity and Coverage Control in Backbone-Based Wireless Networks," *J. Ad Hoc Networks*, vol. 7, pp. 614-621, 2009.
- [12] J. Llorca, S.D. Milner, and C.C. Davis, "A Convex Optimization Method for Autonomous Self-Organization in Dynamic Wireless Networks," *Proc. IEEE Military Comm. Conf. (MILCOM)*, Nov. 2008.
- [13] E.B. Wilson, J.C. Decius, and P.C. Cross, *Molecular Vibrations: The Theory of Infrared and Raman Vibrational Spectra*. McGraw-Hill, 1955.
- [14] Q. Liu, X. Jia, and Y. Zhou, "Topology Control for Multi-Channel Multi-Radio Wireless Mesh Networks Using Directional Antennas," *Wireless Networks*, vol. 17, pp. 41-51, doi:10.1007/s11276-010-0263-1, 2010.
- [15] M. Grossglauser and D.N.C. Tse, "Mobility Increases the Capacity of Ad Hoc Wireless Networks," *IEEE/ACM Trans. Networking*, vol. 10, no. 4, pp. 477-486, Aug. 2002.
- [16] C. Reynolds, "Flocks, Herds, and Schools: A Distributed Behavioral Model," *Computer Graphics*, vol. 21, no. 4, pp. 25-34, 1987.
- [17] C. Reynolds, "Steering Behaviors for Autonomous Characters," *Proc. Game Developers Conf.*, pp. 763-782, 1999.
- [18] A.V. Moore, "Information Flocking: Time-Varying Data Visualization Using Boid Behaviors," *Proc. Eighth Int'l Conf. Information Visualization*, pp. 409-414, 2004.
- [19] G. Proctor and C. Winter, "Information Flocking: Data Visualization in Virtual Worlds Using Emergent Behaviours," *Proc. First Int'l Conf. Virtual Worlds*, pp. 168-176, 1998.
- [20] G. Folino and G. Spezzano, "SPARROW: A Spatial Clustering Algorithm Using Swarm Intelligence," *Applied Informatics (AIA '03)*, pp. 50-55, 2003.
- [21] X. Cui, J. Gao, and T.E. Potok, "A Flocking Based Algorithm for Document Clustering Analysis," *J. Systems Architecture*, vol. 52, pp. 505-515, 2006.
- [22] F. Picarougne et al., "A New Approach of Data Clustering Using a Flock of Agents," *Evolutionary Computation*, vol. 15, no. 3, pp. 345-367, 2007.
- [23] T. Vicsek et al., "Novel Type of Phase Transition in a System of Self-Driven Particles," *Physical Rev. Letters*, vol. 75, no. 6, pp. 1226-1229, 1995.
- [24] A. Jadbabaie, J. Lin, and A.S. Morse, "Coordination of Groups of Mobile Autonomous Agents Using Nearest Neighbor Rules," *IEEE Trans. Automatic Control*, vol. 48, no. 6, pp. 988-1001, June 2003.
- [25] L. Moreau, "Stability of Multiagent Systems with Time-Dependent Communication Links," *IEEE Trans. Automatic Control*, vol. 52, no. 2, pp. 169-182, Feb. 2005.
- [26] V. Gazi and K.M. Passino, "Stability Analysis of Swarms," *IEEE Trans. Automatic Control*, vol. 48, no. 4, pp. 692-697, Apr. 2003.
- [27] V. Gazi and K.M. Passino, "Stability Analysis of Social Foraging Swarms," *IEEE Trans. Systems, Man, and Cybernetics-Part B: Cybernetics*, vol. 34, no. 1, pp. 539-557, 2004.
- [28] I.D. Couzin, "Effective Leadership and Decision Making in Animal Groups on the Move," *Nature*, vol. 433, pp. 513-516, 2005.
- [29] H.T. Zhang and G. Chen, "Small-World Network-Based Coordinate Predictive Control of Flocks," *Proc. IEEE Third Int'l Scientific Conf. Physics and Control*, 2007.
- [30] J. Kennedy and R.C. Eberhart, "Particle Swarm Optimization," *Proc. IEEE Int'l Conf. Neural Networks (ICNN '95)*, pp. 1942-1948, Nov./Dec. 1995.
- [31] A.P. Engelbrecht and A. Ismail, "Training Product Unit Neural Networks," *Stability and Control: Theory and Applications*, vol. 2, nos. 1/2, pp. 59-74, 1999.
- [32] M. Omran, A.P. Engelbrecht, and A. Salman, "Particle Swarm Optimization Method for Image Clustering," *Int'l J. Pattern Recognition and Artificial Intelligence* vol. 19, no. 3, pp. 297-321, 2005.
- [33] C. Grosan, A. Abraham, and M. Chis, "Swarm Intelligence in Data Mining," *Studies in Computational Intelligence*, vol. 34, pp. 1-20, 2006.
- [34] C.-F. Juan and C.-H. Hsu, "Temperature Control by Chip-Implemented Adaptive Recurrent Fuzzy Controller Designed by Evolutionary Algorithm," *IEEE Trans. Circuits and Systems I: Regular Papers*, vol. 52, no. 11, pp. 2376-2384, Nov. 2005.

- [35] J. Park, K. Choi, and D.J. Allstot, "Parasitic-Aware RF Circuit Design and Optimization," *IEEE Trans. Circuits and Systems I: Regular Papers*, vol. 51, no. 10, pp. 1953-1966, Oct. 2004.
- [36] Y. Shi and R.C. Eberhart, "Empirical Study of Particle Swarm Optimization," *Proc. Congress Evolutionary Computation*, pp. 1945-1949, 1999.
- [37] T.S. Rappaport, *Wireless Communications: Principles and Practice*, pp. 69-196, Prentice-Hall, 1996.
- [38] V. Gazi and K.M. Passino, "Stability Analysis of Swarms," *Proc. Am. Control Conf.*, pp. 1813-1818, May 2002.
- [39] J. Llorca, A. Desai, and S.D. Milner, "Obscuration Minimization in Dynamic Free Space Optical Networks Through Topology Control," *Proc. IEEE Military Comm Conf. (MILCOM)*, vol. 3, pp. 1247-1253, 2004.
- [40] T. Cormen, C. Leiserson, and R. Rivest, *Introduction to Algorithms*, first ed. MIT, 2001.
- [41] X. Hong, M. Gerla, G. Pei, and C.-C. Chiang, "A Group Mobility Model for Ad Hoc Wireless Networks," *Proc. Second ACM Int'l Workshop Modeling, Analysis and Simulation of Wireless and Mobile Systems*, pp. 53-60, 1999.
- [42] D.B. Shmoys, E. Tardos, and K. Aaradalz, "Approximation Algorithms for Facility Location Problems," *Proc. ACM Symp. Theory of Computing (STOC)*, May 1997.



Haijun Zhang received the BEng degree and the master's degree from the Northeastern University, Shenyang, P.R. China, in 2004 and 2007, respectively, and the PhD degree in the Department of Electronic Engineering from City University of Hong Kong in 2010. From 2010 to 2011, he was a postdoctoral research fellow in the Department of Electrical and Computer Engineering at the University of Windsor, Canada. Since 2012, he has been at the Shenzhen

Graduate School of the Harbin Institute of Technology, Shenzhen, P.R. China, where he is currently an associate professor of Computer Science. His research interests include multimedia data mining, machine learning, pattern recognition, evolutionary computing, and communication networks.



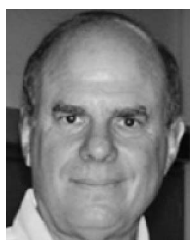
Jaime Llorca received the BS degree in electrical engineering from the Polytechnic University of Catalunya, Barcelona, Spain, in 2001, and the MS and PhD degrees in electrical and computer engineering from the University of Maryland, College Park, in 2003 and 2008, respectively. Currently, he is working as a communication networks research scientist at Alcatel-Lucent Bell Labs, Holmdel, New Jersey. His research interests include energy efficiency

in communication networks, optical communications, content distribution networks, topology control, self-organization, and network optimization. He is a member of the IEEE.



Christopher C. Davis received the BA degree in natural sciences in 1965 and the MA degree in 1970 from the University of Cambridge, and the PhD degree in physics from the University of Manchester in 1970. His PhD thesis work was on the fundamental processes that occur in gaseous noble gas lasers. From 1973 to 1975, he was a research associate at Cornell University working on processes important in chemical lasers. Since 1975, he has been at

the University of Maryland, College Park, where he is currently a professor of electrical and computer engineering. From 1982-1983, he was a senior visiting fellow at the University of Cambridge. His current research interests include optical wireless communication systems, sensor nets, nano-optics, plasmon optics, near-field scanning optical microscopy, fiber sensors, biosensors, and characterization of antennas in the near field. He is author of the text *Lasers and Electro-Optics* and coauthor of the best-selling text *Building Scientific Apparatus*, now in its fourth edition, both published by Cambridge University Press. He is a fellow of the Institute of Physics and a member of both the Optical Society of America, SPIE, and the IEEE.



Stuart D. Milner received the BS degree from the University of Maryland, the MS degree from the University of Georgia, and the PhD degree from the University of Pittsburgh. Currently, he is working as a research professor in the Department of Civil and Environmental Engineering and director of the Center for Networking of Infrastructure Sensors, University of Maryland, College Park. His research projects and interests include sensor networks, dynamic topology

control, adaptive mobile networks, network science, and network enabled systems. Previously, he was a program manager in the Defense Advanced Research Projects Agency, where he directed research and development programs in advanced networking technologies, large-scale simulation networks, and wireless network technologies. He is a member of the IEEE.

► For more information on this or any other computing topic, please visit our Digital Library at www.computer.org/publications/dlib.